# Dissociation energies of the hydrogen and deuterium molecules

A. Balakrishnan,* V. Smith,† and B. P. Stoicheff
*Department of Physics, University of Toronto, Toronto, Ontario, Canada M5S 1A7*
*and Ontario Laser and Lightwave Research Centre, Toronto, Ontario, Canada M5S 1A7*
(Received 30 September 1993)

Fluorescence-excitation spectroscopy near ~84 nm has been used to measure the threshold for the dissociation of $H_2(B'\,^1\Sigma_u^+)=H(1s)+H(2s)$ at 118 377.06±0.04 $cm^{-1}$ and the corresponding limit for $D_2$ at 119 029.72±0.04 $cm^{-1}$. The onset of dissociation was observed clearly, free from overlapping molecular lines, by the use of delayed quenching of 2*s* atoms produced by the photoexcitation pulse. These measurements have yielded the values $D_0(H_2)=36\,118.11\pm0.08$ $cm^{-1}$ and $D_0(D_2)=36\,748.38\pm0.07$ $cm^{-1}$ for the dissociation energies of the ground electronic states $X\,^1\Sigma_g^+$, in agreement with the latest *ab initio* calculations, which include nonadiabatic, relativistic, and radiative corrections. From the present values and recently determined ionization energies of $H_2$ and $D_2$, the dissociation energies of the respective ions were found to be $D_0(H_2^+)=21\,379.37\pm0.08$ $cm^{-1}$ and $D_0(D_2^+)=21\,711.64\pm0.07$ $cm^{-1}$, also in agreement with recent *ab initio* calculations.

PACS number(s): 35.20.Gs, 33.20.Ni, 32.50.+d

## I. INTRODUCTION

The determination of the dissociation energies of $H_2$, HD, and $D_2$, the simplest neutral molecules, has been recognized as a fundamental problem in molecular physics since the beginning of quantum mechanics. Significant reductions in experimental and theoretical uncertainties have taken place since 1960 when Herzberg and Monfils [1] obtained improved extreme-ultraviolet (XUV) absorption spectra of these molecules. However, until recently, there has been a difference of 0.3–0.7 $cm^{-1}$ between *ab initio* and experimental values of the dissociation energies, the calculated values being the lower for all three isotopes. The recent *ab initio* values of the dissociation energies, by Wolniewicz [2] (that include relativistic, radiative, and nonadiabatic corrections to the Born-Oppenheimer approximation and are estimated to have an accuracy of ±0.01 $cm^{-1}$), reaffirm this discrepancy. Moreover, the corrections are small and range in value from 0.2 to 0.5 $cm^{-1}$. Thus experimental precision better than 0.2 $cm^{-1}$ is required to confidently test the theory in all its aspects. At least two groups have carried out investigations towards this end, both taking advantage of recent advances in laser spectroscopy: McCormack and Eyler [3] began high-resolution studies with double-resonance laser techniques, while we have used single-photon fluorescence-excitation spectroscopy with tunable radiation near 84 nm [4].

In most of the previous experiments, as in the present work, the ground-state dissociation energy has been derived from measurements of the second dissociation limit ($D_L$) of molecular hydrogen in the $B'\,^1\Sigma_u^+$ state, which dissociates into an atom in the 1*s* ground level and one in the 2*s* excited level. The ground-state dissociation energy is then obtained by subtracting the atomic excitation energy from $D_L$, as illustrated in Fig. 1. In 1970, Herzberg [5] reinvestigated the absorption spectra of $H_2$, HD, and $D_2$ at 77 K, with even higher resolution using a 10.5-m vacuum spectrograph. For $H_2$, intense molecular lines in the region of the dissociation limit obstructed a clear view of the dissociation threshold. However, upper and lower bounds for the limit were obtained, and Herzberg favored the upper bound, yielding a value of $D_0(H_2)=36\,118.3$ $cm^{-1}$. For $D_2$, the limit was free of overlapping lines, and a reliable value of $D_0(D_2)=36\,748.9\pm0.4$ $cm^{-1}$ was obtained. At that time, Stwalley [6] made new vibrational assignments of the molecular lines near the limit and by extrapolation based on the long-range behavior of the internuclear potential energy of the $B\,^1\Sigma_u^+$ state, obtained a dissociation energy of

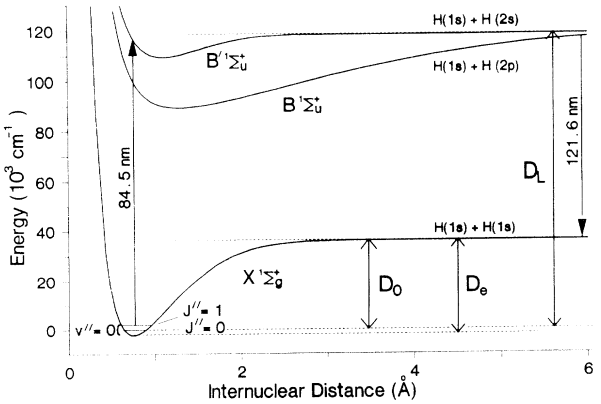


FIG. 1. Energy-level diagram showing the ground $X(^1\Sigma_g^+)$ and excited states $B(^1\Sigma_u^+)$ and $B'(^1\Sigma_u^+)$ of $H_2$. The fluorescence-excitation scheme for determining the second dissociation threshold $D_L(H_2)$ and the dissociation energies $D_0(H_2)$ and $D_e(H_2)$ is indicated.

*Present address: National Institute of Standards and Technology, Physics 221, Rm. A253, Gaithersburg, MD 20899.
†Permanent address: Université de Rennes, Département de Physique Atomique et Moléculaire, Campus de Beaulieu, 35042 Rennes Cedex, France.

 

$D_0(H_2)=36\,118.6\pm0.5$ cm$^{-1}$. In 1975, LeRoy and Barwell [7] determined a value of $D_0(D_2)=36\,748.88\pm0.3$ cm$^{-1}$ from the first rotational term value of the ground-state vibrational level $v=21$ [8], only 2 cm$^{-1}$ from the dissociation limit. McCormack and Eyler [3] reinvestigated the spectrum of molecular lines of $H_2$ near the second dissociation limit, at very high resolution, and observed a complex structure of lines which differed from the predicted spectrum. These authors concluded that a better theoretical understanding of the perturbed spectrum is necessary for a precise determination of the limit from the extrapolation of the energies of high vibrational levels. In addition, they observed the threshold of the second dissociation continuum at $118\,377.23\pm0.20$ cm$^{-1}$, yielding the value $D_0(H_2)=36\,118.26\pm0.20$ cm$^{-1}$. Recently, Eyler and Melikechi [9] have reported on improved determinations of the dissociation limits of $H_2$, HD, and $D_2$, giving $D_0(H_2)=36\,118.06\pm0.04$ and $D_0(D_2)=36\,748.32\pm0.07$ cm$^{-1}$.

In our earlier papers, we have reported briefly on the observations and measurements of the thresholds of the second dissociation continua of $H_2$ and $D_2$ based on fluorescence-excitation spectra at 84–84.5 nm [4,10]. These have yielded the values $D_0(H_2)=36\,118.11\pm0.08$ cm$^{-1}$ and $D_0(D_2)=36\,748.38\pm0.07$ cm$^{-1}$, in good agreement with the *ab initio* calculations of Wolniewicz [2], $36\,118.060\pm0.01$ and $36\,748.355\pm0.01$ cm$^{-1}$, respectively. Thus, for the first time since the earliest experiments and calculations of the dissociation energy of hydrogen in 1926 and 1927, respectively [11,12], the experimental and theoretical values are in agreement within the small uncertainties of the experimental values. In the present paper, we report in detail on the experimental results obtained for the dissociation energies of both $H_2$ and $D_2$.

## II. EXPERIMENTAL METHOD

An outline of the experimental arrangement used for generating tunable XUV radiation in the region of 84–84.5 nm and for investigating absorption and fluorescence-excitation spectra of $H_2$ and $D_2$ is shown in Fig. 2. Pulsed radiation from two dye lasers was combined in Kr gas to generate XUV radiation by four-wave sum mixing (4WSM) and this radiation excited $H_2$ or $D_2$ in a pulsed jet of the sample gas. Any metastable $2s$ atoms produced in the photodissociation process were quenched by an electric field applied after the excitation pulse, and fluorescence in the Lyman-$\alpha$ region was measured as the XUV radiation was tuned in frequency. The apparatus and technique that provided a clear observation of the photodissociation threshold of $H_2$ and $D_2$ are described below.

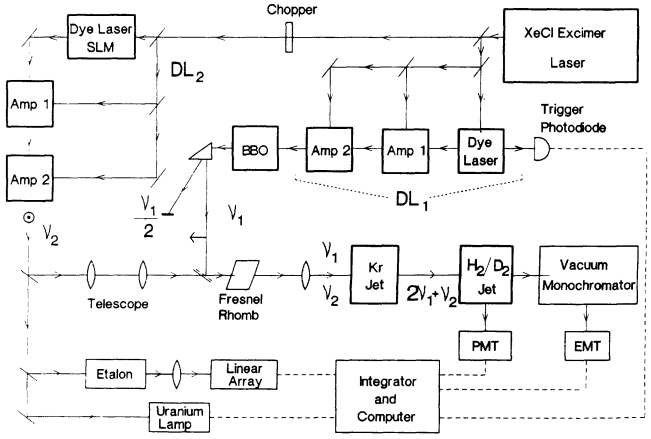


FIG. 2. Schematic diagram of the experimental arrangement.

### A. Laser sources

The primary radiation source was a XeCl excimer laser (Lumonics TE-861M-2) with unstable resonator optics, operating at 308 nm, in pulses of 50 mJ and a 7-Hz repetition rate. This radiation was segmented into two beams of equal intensity for pumping the dye-laser systems $DL_1$ and $DL_2$, each of which consisted of an oscillator and two amplifiers, and provided tunable radiation at frequencies $\nu_1/2$ and $\nu_2$, respectively. For $DL_1$, ~15% of the incident laser power was allotted to the oscillator and ~30% and 55% to the preamplifier and amplifier, respectively. For $DL_2$, the respective pump powers were ~5%, 35%, and 60%. The oscillator of $DL_1$ was a commonly used system in this laboratory, consisting of a double-grating grazing-incidence configuration [13] and was pumped transversely to generate radiation at ~425 nm in 3-ns pulses, with a bandwidth of ~0.2 cm$^{-1}$. This radiation was amplified to peak powers of 100 kw and frequency doubled in a $\beta$-barium borate crystal BBO (CSK Co.), 6.5 mm long with 4 mm × 4 mm face, to generate radiation at ~212.6 nm with a peak power of ~15 kW. The fundamental ($\nu_1/2$) and second-harmonic ($\nu_1$) beams were separated by a fused silica prism.

For $DL_2$, the oscillator of a single-longitudinal mode (SLM) dye laser [14] (Lumonics HyperDye-SLM) was used along with two transversely pumped amplifier cells of homemade design (the same as in $DL_1$) to generate radiation over the wavelength range 400–425 nm. It was noted that the beam emitted by the oscillator consisted of two pulses, each ~2 ns in duration, separated by ~4 ns; this profile arose from a ripple in the pulse of the XeCl excimer laser. Best results in single-mode operation were obtained with an incident beam energy of ~1 mJ/pulse and beam spot size of 300–600 $\mu$m for longitudinal pumping at the oscillator cell. Also, the delay of the amplifier pump beams, initially set to amplify the first pulse, was extended another 4 ns in order to amplify only the second pulse from the SLM oscillator. In this way, single-mode operation of $DL_2$ with peak powers of ~55 kW and bandwidth of ~0.02 cm$^{-1}$ was achieved over a tuning range ~80 cm$^{-1}$. The range deteriorated to ~20 cm$^{-1}$ in a few days of operation, still sufficient for the present experiments. A Fabry-Pérot etalon having a 1-cm$^{-1}$ free-spectral range was used with a linear array detector (Spiricon SILP-1024-025W/L) to monitor single-mode operation of $DL_2$ during each experiment. A small portion of the $DL_2$ beam was also diverted to a uranium hollow-cathode lamp with either Ar or Ne buffer gases (Buck Scientific or Westinghouse) for fre-

TABLE I. Dye concentrations and solvents.

| Wavelength (nm) | Laser | Dye | Molar concentration (mol/l) | Solvent |
|---|---|---|---|---|
| 401–402 | $DL_2$(Osc.) | Exalite 398 | $6.2\times10^{-4}$ | *p*-dioxane |
| | $DL_2$(Amp.) | Exalite 398 | $3.1\times10^{-4}$ | *p*dioxane |
| 404 | $DL_2$(Osc.) | Exalite 404 | $7.4\times10^{-4}$ | *p*-dioxane |
| | $DL_2$(Amp.) | Exalite 404 | $3.7\times10^{-4}$ | *p*-dioxane |
| 412–414 | $DL_2$(Osc.) | Exalite 416 | $1.6\times10^{-3}$ | *p*-dioxane |
| | $DL_2$(Amp.) | Exalite 416 | $2.7\times10^{-4}$ | *p*-dioxane |
| 425 | $DL_2$(Osc.) | Stilbene 420 | $1.0\times10^{-3}$ | methanol |
| | $DL_1$(Osc.) | Stilbene 420 | $1.4\times10^{-3}$ | 90% ethanol, 10% water |
| | $DL_1$(Amp.) | Stilbene 420 | $7.0\times10^{-4}$ | 90% ethanol, 10% water |

quency calibration of $\nu_2$ as the oscillator was scanned.

The dyes used in the oscillators and amplifiers, with their solvents and concentrations, are listed in Table I. All dyes were obtained from the Exciton Corp., and the high-grade solvents of methanol, ethanol, and 1,4 *p*-dioxane from Fisher Scientific. Distilled water was used throughout.

### B. Generation of tunable XUV radiation at 84–84.5 nm

The required monochromatic XUV radiation, tunable in the region 84–84.5 nm, was generated by the standard method of four-wave frequency mixing [15], with $\nu_1$ tuned to a two-photon resonance ($2\nu_1$) in Kr, and $\nu_2$ freely variable to produce tunable radiation at $2\nu_1+\nu_2$. Our use of a jet of Kr gas was adapted from the work of Hilber, Lago, and Wallenstein [16], who found Kr to be an efficient nonlinear medium for generation in the 80-nm region.

The chamber for XUV generation consisted of a stainless-steel cross with six ports of 10 cm diameter (Dependex) and was maintained at a pressure $<1$ mTorr by a mechanical pump (Edwards E2M40). A nozzle of 1 mm diameter (Laser Technics LPV) was mounted at the top to produce a vertical effusive beam of Kr gas, and two electrodes were placed beneath the nozzle for collection and measurement of $Kr^+$ ions. The jet was pulsed to economize on Kr gas and to permit adequate evacuation of the chamber with medium pump capacity in order to avoid reabsorption of the generated XUV radiation. The pulse of Kr gas was synchronized to the $\nu_1$ and $\nu_2$ excitation pulses. A window of fused silica transmitted the incident $\nu_1$ and $\nu_2$ radiation while at the opposite end, a 3-mm-diam aperture in a Plexiglas barrier permitted the entry of the XUV radiation into the $H_2$-$D_2$ sample chamber.

Initially, the $\nu_1$ beam was aligned to define the optical axis by sending it through apertures to enter the Kr jet and sample chambers. The beam was then focused by a lens of 25 cm focal length and the Kr nozzle was brought to a point $\sim0.5-1$ mm above the focus, a region having the highest gas density. Next, the oscillator of $DL_1$ was tuned until a strong $Kr^+$ ion signal was detected, arising from two-photon resonantly enhanced three-photon ionization. In this way, the frequency $\nu_1$ was set so that $2\nu_1$ was resonant with the level $4p^5 5p[\frac{1}{2}]_0$ of Kr. Following this initial tuning of $\nu_1$, the frequency setting was optimized by detection of third-harmonic generation with a 1-m vacuum spectrometer (McPherson 225) and an electron multiplier (ITT F4074). Next, the $\nu_2$ beam was synchronized to within 0.3 ns and overlapped with the $\nu_1$ beam at a dichroic mirror (Acton Research 212/V-FR45-1D-FL). A 1:1 telescope was inserted into the $\nu_2$-beam path just before the dichroic mirror to compensate for dispersion of $\nu_1$ and $\nu_2$ radiation in the focusing lens. Finally, the beam overlap was optimized by maximizing the 4WSM strength. Beam alignment was required daily. Optimum generation of XUV radiation in pulses of $\sim4$-ns duration with peak powers estimated to be $\sim100$ mW, was achieved for incident $\nu_1$ and $\nu_2$ intensities of $\sim8\times10^8$ and $\sim2\times10^9$ W/cm$^2$, respectively, and for Kr backing pressures of $\sim2$ atm. A bandwidth of 0.25 cm$^{-1}$ was realized, representing a resolving power of $\sim5\times10^5$ in the XUV.

### C. $H_2$-$D_2$ chamber with quenching field and detection optics

The sample chamber was identical to the Kr chamber and immediately followed it, the two being separated by a Plexiglas barrier having a 3-mm-diam aperture for entry of the XUV beam. A pulsed jet (Laser Technics LPV) with a nozzle of 1 mm diameter was placed on top of the chamber and operated with $H_2$ (or $D_2$) at a backing pressure of 5.5 atm. The chamber was pumped from below by a diffusion pump (TM-Vacuum Products 641) backed by a mechanical pump and maintained at a vacuum of $\sim10^{-5}$ Torr.

The jet nozzle was positioned so that the XUV radiation interacted with the $H_2$ (or $D_2$) effusive beam in the region of supersonic expansion, $\sim50$ mm below the nozzle. A view of this part of the chamber is shown in Fig. 3. Fluorescence radiation was collected by a concave aluminum mirror (5 cm diameter and 7.6 cm radius of curvature, with $MgF_2$ coating, Acton Research 1200) positioned with its axis perpendicular to the incident XUV beam to image a small central section ($\sim1.2$ mm diame-

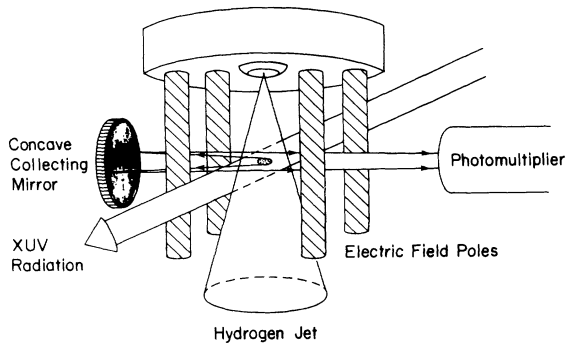


FIG. 3. View of the chamber where XUV radiation interacts with the vertical hydrogen beam effusing from a jet nozzle. The concave collecting mirror and quenching field electrodes are also shown.

ter) of the interaction region on the photocathode of a solar-blind photomultiplier (EMR 541G-08-17). In this way, the Doppler breadth arising from the conical expansion of the $H_2$ jet was significantly reduced. Four aluminum posts spaced 4 cm apart permitted the application of a dc electric field of 50–150 V/cm for quenching of the $2s$ metastable atoms produced in the photodissociation process. The electric field was switched on by a silicon controlled rectifier (International Rectifier 16RIA120) having a rise time of $\sim$800 ns. In the later experiments with $D_2$, a power metal-oxide-semiconductor field-effect transistor (MOSFET) (International Rectifier IRFPG50) with $\sim$100 ns rise time became available and replaced the rectifier.

Signals from the photomultiplier or electron multiplier, uranium lamp, and linear-array detector were all sampled simultaneously by gated integrators and recorded digitally with a computer interface (Stanford Research System SR250 and SR245). The 1-m vacuum spectrometer (McPherson 225) with electron multiplier (ITT F4074) was also used for observation of absorption spectra, for monitoring the intensity of XUV radiation, and for establishing the two-photon resonance in Kr, in a separate experiment, described at the end of Sec. II D.

### D. Investigation of the fluorescence-excitation spectra of $H_2$ and $D_2$

Initially, absorption as well as fluorescence-excitation spectra of $H_2$ were obtained under a variety of conditions as the experimental technique was gradually optimized. Spectra were recorded as the XUV frequency was scanned through the higher vibronic levels of the $B$ and $B'$ states and into the second dissociation continuum. However, the threshold region was obscured by overlapping molecular lines, despite significant improvement in resolution which only served to reveal finer features in each line. Later, spectra were recorded at lower densities to eliminate collisional quenching of metastable atoms and a delayed electric field was introduced to quench the dissociation products.

In order to determine the proper timing and duration of the electric field, temporal measurements of the fluorescence intensity were taken with a calibrated transient digitizer (Tektronix 7912AD) using the power MOSFET. This study was performed in the region of the second dissociation limit of $H_2$ with $J''=1$, well suited for the experiment because of the large number of molecular lines and the strong continuum. It is known that the $2p$ level has a lifetime of 1.6 ns, and the molecular levels giving rise to the lines overlapping the threshold region were found to decay faster than the instrumental response time ($\sim$10 ns). For $H_2$, in the absence of electric fields, the fluorescence intensity of the dissociation continuum showed a single exponential decay caused by collisional quenching of $2s$ atoms by $H_2$. This decay time increased with increasing distance of the interaction region from the $H_2$ jet nozzle, and a lifetime of 516$\pm$10 ns was measured for a distance of 50 mm. With the application of a quenching field of $\sim$50 V/cm, the metastable atoms decayed within 300 ns. Thus, after a delay of a few hundred nanoseconds, quenched fluorescence was observed long after decays of bound molecular states had occurred.

Once optimum conditions were established, spectra were repeatedly scanned over a 15-cm$^{-1}$ region centered about the onset of the dissociation threshold, at a scanning rate of 0.03 cm$^{-1}$/sec, with the lasers pulsed at 7 Hz. (Scattered $\nu_1$ radiation produced an appreciable background signal, so the $DL_2$ pump beam was blocked in alternate pulses to allow background subtraction). For each scan, the electric field was zero during the XUV pulse ($\sim$4-ns duration) and triggered 10–30 ns later. The fluorescence was sampled from 200–800 ns after switching on the field with the rectifier (rise time $\sim$800 ns) and from $\sim$100 ns when using the MOSFET (rise time $\sim$100 ns). The signal-to-noise ratio (SNR) for the first few scans was $\sim$4, and each spectral region was scanned repeatedly until the SNR dropped to $\sim$1 (over a period of $\sim$3 h). Simultaneously, uranium spectra were obtained using the optogalvanic effect, with $\sim$4–8 sharp lines (bandwidth $\sim$0.06 cm$^{-1}$) being recorded over the 15-cm$^{-1}$ intervals for calibration of $\nu_2$ [17]. Each scan was examined before analysis; some were discarded if the étalon traces indicated multimode operation or mode hopping of $DL_2$, or if the uranium spectrum showed irreproducible behavior arising from fluctuations in the lamp discharge. Of the 15–20 scans in an experimental run, usually 10–15 scans were suitable for analysis. These scans were overlapped by maximizing the cross correlation of the uranium scans and summed in order to improve the SNR. Before summing, each scan was normalized by its power content (the root-mean-square value of the scan's amplitude) in order to compensate for changes to the photomultiplier tube gain or amplifier settings and to give higher weight to scans with better SNR. Finally, the fluorescence-excitation spectra and uranium spectra were digitally smoothed with a Gaussian filter of 0.04 cm$^{-1}$ bandwidth. In this way, spectra of the threshold regions were obtained for $H_2$ in the $J''=0$ and 1 levels and for $D_2$ in the $J''=0$, 1, and 2 levels. While these levels were sufficiently populated to provide detectable spectra, the spectra for ortho-$H_2$ ($J''=1$) and ortho-$D_2$ ($J''=0$) were superior in every way, since these levels are the most highly populated in $H_2$ and $D_2$, respectively.

For determination of the frequency scale in each spectrum, the fixed frequency $2\nu_1$ was measured and added to $\nu_2$. Recall that $2\nu_1$ is the energy of the $4p^5 5p\,[\frac{1}{2}]_0$ level of Kr used for the two-photon resonance enhancement. For this measurement, a separate experiment was carried out, replacing dye laser $DL_1$ with the SLM laser $DL_2$ because of the much narrower linewidth of $DL_2$. This laser beam was set to operate at $\nu_1/2$ and at the same intensity as the original beam from $DL_1$, then frequency doubled, and sent through the identical path followed by radiation from $DL_1$ in the photoexcitation experiments. The frequency was tuned while observing the third-harmonic signal (near 70.9 nm), which was sampled by a gated integrator and stored together with a uranium spectrum for calibration of $\nu_1/2$. Two separate measurements yielded the value $\nu_1/2 = 23\,523.25 \pm 0.01$ cm$^{-1}$, giving $94\,093.00 \pm 0.04$ cm$^{-1}$ for $2\nu_1$ and for the energy of the $4p^5 5p\,[\frac{1}{2}]_0$ level of Kr. In this way, the $H_2$ and $D_2$ spectra were calibrated as a function of the XUV frequency $2\nu_1 + \nu_2$.

## III. RESULTS AND ANALYSIS

### A. Hydrogen

#### 1. *Dissociation spectrum of ortho-$H_2$ ($J''=1$)*

One of the first fluorescence-excitation spectra of ortho-$H_2$ in the region of the second dissociaton limit recorded in the present experiments is shown in Fig. 4. This spectrum was obtained at an effective resolution of 0.7 cm$^{-1}$, at relatively high gas density (with the interaction region ~5 mm from the jet nozzle), by sampling the fluorescence with a short gate (several nanoseconds in duration), immediately after the photoexcitation pulse. No quenching electric field was applied. At such high densities, any metastable H(2$s$) atoms are quenched quickly by collisions, and all products of photoexcitation, including H(2$s$) and H(2$p$) atoms, as well as $H_2$ in high vibronic levels, decay by fluorescence within a few nanoseconds. Thus the spectrum exhibits many molecular lines which overlap the onset of the dissociation continuum and limit the accuracy of determining the second dissociation threshold $D_L$. With the resolution improved to 0.25 cm$^{-1}$, and with the interaction region ~20 mm from the nozzle, all other conditions being the same, the spectrum of Fig. 5(a) was obtained. The most prominent features are the molecular lines, while the intensity of the dissociation continuum is barely discernible. With the application of an electric field to quench the H(2$s$) atoms and by extending the sampled duration to ~750 ns to include fluorescence synchronous with this field, the spectrum of Fig. 5(b) was recorded, showing a somewhat more intense dissociation continuum and the prominent molecular lines.

Finally, the spectrum of quenched fluorescence alone was obtained at a distance of 50 mm from the nozzle.

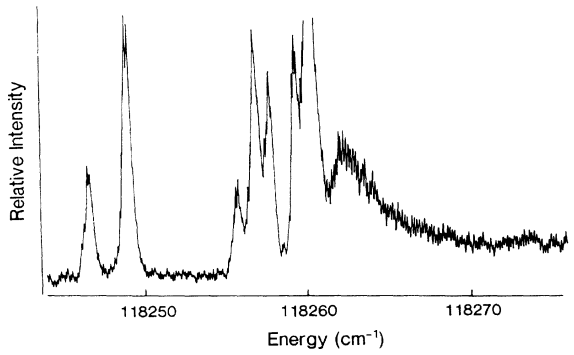


FIG. 4. A fluorescence-excitation spectrum in the region of the second dissociation limit of ortho-$H_2$ ($J''=1$), recorded with a resolution of ~0.7 cm$^{-1}$. The spectrum was obtained by sampling for a short time the fluorescence ~5 mm below the jet nozzle, immediately after excitation, and without the application of the quenching field.

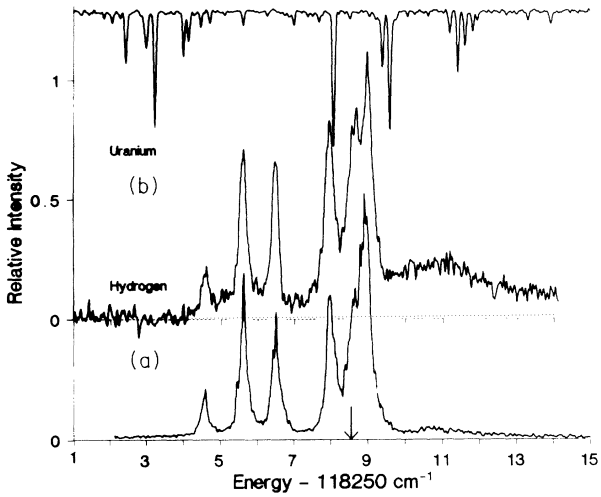


FIG. 5. Spectra near the second dissociation limit of ortho-$H_2$, obtained at a resolution of ~0.25 cm$^{-1}$ and ~20 mm below the jet nozzle: (a) recorded without a quenching field and using a gated integrator to sample the fluorescence coincident with the photoexcitation pulse; (b) recorded with a delayed quenching field and including the quenched fluorescence synchronous with the field. The uppermost spectrum is that of uranium used to calibrate the scanning frequency $\nu_2$.

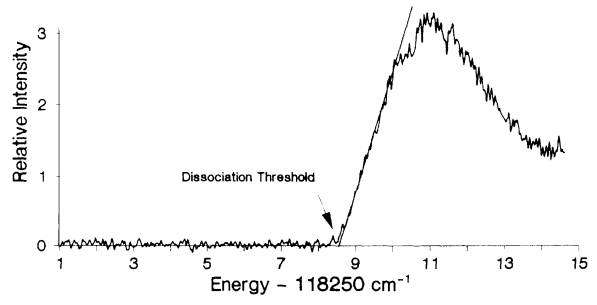


FIG. 6. Spectrum of the second dissociation limit of ortho-$H_2$ recorded while sampling only the fluorescence of quenched H(2$s$) atoms ~50 mm below the jet nozzle. The spectrum was obtained with the application of an electric field 10–30 ns after the photodissociation pulse, and signal detection (synchronously with the field) delayed by 200 ns with respect to the photoexcitation pulse, and using a gate width of 500 ns.

Such a spectrum is shown in Fig. 6. There is no evidence of molecular features and the onset of the photodissociation continuum is clearly revealed. The intensity of the continuum increases linearly, with some structure evident within the first wave number of the continuum; it reaches a maximum at $\sim 2$ cm$^{-1}$ above threshold, then drops to a relatively constant value which is maintained over a region $>120$ cm$^{-1}$. A value of $D_L(H_2)=118\,258.57$ cm$^{-1}$ was determined for the second dissociation limit by linear extrapolation, with an accuracy of $\pm 0.04$ cm$^{-1}$. This result is the weighted average of two runs consisting of 10–15 scans (Sec. II D), each of which exhibited the features described above.

#### 2. *Dissociation spectrum of para-$H_2$ ($J''=0$)*

The spectrum of quenched fluorescence in the vicinity of the second dissociation limit of para-$H_2$ is shown in Fig. 7 along with the spectrum of molecular lines (shown by the dotted line) obtained from the immediate fluorescence and no field. While the onset of the photodissociation continuum is evident, the spectrum lies atop a strong background arising from the dissociation of ortho-$H_2$, and a prominent dip in this background complicates the analysis of the spectrum. This feature is thought to arise from absorption of the incident XUV radiation by the transitions near 118 376 cm$^{-1}$, which are shown by the dotted line in Fig. 7. The breadth of this feature is indicative of the Doppler broadening across the full conical expansion of the jet plume. A linear extrapolation indicates a value of $\sim 118\,377.0$ cm$^{-1}$ for the threshold, but the accuracy is limited by the broad absorption.

#### 3. *The dissociation energy $D_0(H_2)$ and $D_e(H_2)$ of hydrogen*

The spectrum of Fig. 6 gives the value $118\,258.57\pm 0.04$ cm$^{-1}$ for the second dissociation limit, above the energy of the $J''=1$ level of the ground state. To obtain the dissociation limit with respect to the lowest level $J''=0$, the first rotational term value, namely, $F''(1)=118.49$ cm$^{-1}$ [18], was added, giving $D_L(H_2)=118\,377.06\pm 0.04$ cm$^{-1}$. (The estimate obtained from the spectrum of para-$H_2$ agrees with this value.) Finally, the dissociation energy of $H_2$ in the ground state was derived by subtracting from $D_L(H_2)$, the energy interval $E(2s)-E(1s)=82\,258.954$ cm$^{-1}$ [19], to give

$$D_0(H_2)=36\,118.11\pm 0.08 \text{ cm}^{-1} .$$

The error quoted here is discussed in Sec. III C. To this value of $D_0$ we add the zero-point energy of vibration $2179.27\pm 0.05$ cm$^{-1}$ [20] to yield the equilibrium value of the dissociation energy

$$D_e(H_2)=38\,297.38\pm 0.10 \text{ cm}^{-1} .$$

### B. Deuterium

#### 1. *Dissociation spectrum of ortho-$D_2$ ($J''=0$)*

A spectrum of the quenched fluorescence in the vicinity of the second dissociation threshold is shown in Fig. 8, along with a spectrum of the molecular lines, obtained by the procedures described for $H_2$ in Sec. III A 1. The results of three different runs were summed in order to improve the signal-to-noise ratio. The spectrum is superimposed on a background arising from the dissociation continua of molecules initially in the higher rotational levels $J''=1$ and 2. Emission and absorption features corresponding to the molecular lines are also recorded in the dissociation spectrum of Fig. 8. The broad absorption of 119 036 cm$^{-1}$ is due to absorption by the jet plume and the sharp peaks arise from saturation of the photomultiplier (used with high gain) by the intense molecular emission. In order to minimize the intensity of these peaks, the sampling gate of the integrator was further delayed from 200 to 300 ns. Nonetheless, the onset of the photodissociation is clear and free of extraneous features. The continuum rises very sharply to a maximum, within $\sim 0.5$ cm$^{-1}$ and then levels off.

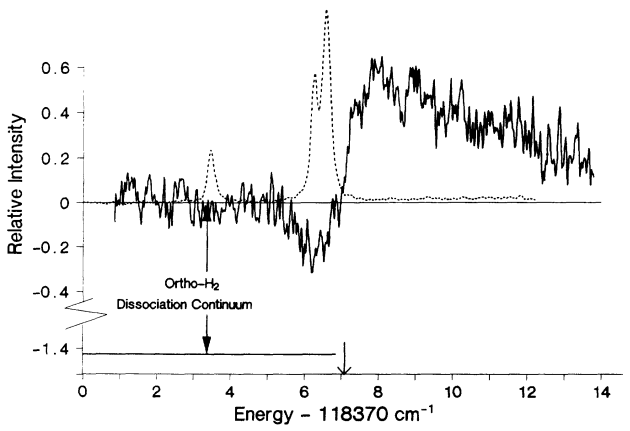


FIG. 7. Spectrum of quenched fluorescence near the second dissociation limit of para-$H_2$ ($J''=0$). The molecular lines (shown by the dotted line) were recorded by sampling the fluorescence immediately after photoexcitation, without the quenching field.

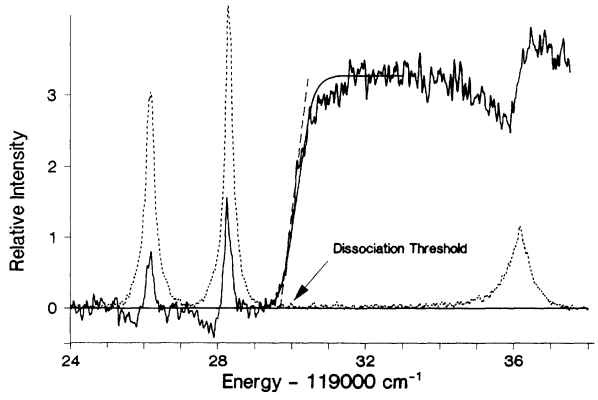


FIG. 8. Spectrum of quenched fluorescence near the second dissociation limit of ortho-$D_2$ ($J''=0$) showing (by the dotted line) the molecular lines in this region recorded without the field. The dashed line is the linear extrapolation to the threshold and the solid line demonstrates the effect of convoluting the slope of this line with the molecular line shape.

As for $H_2$, a linear extrapolation seemed to be warranted and was carried out. However, a slight departure from a linear dependence was noticed at the lowest intensity. This curvature is attributed to the finite spectral resolution whose effect is manifest only for sharper features and was barely noticeable at the $H_2$ threshold (Fig. 6). Thus the observed width (full width at half maximum of 0.25 $cm^{-1}$) of the molecular line at 119 026.23 $cm^{-1}$ was chosen to represent the spectral line shape for convolution with a step function sloped according to the linear fit. The resulting curve matches the observed spectrum at the onset of the continuum, as shown in Fig. 8. From this fit to the observed spectrum, the second dissociation limit was determined to occur at $D_L(D_2)=119\,029.72\pm0.04$ $cm^{-1}$.

### 2. *Dissociation spectra for $J''=1$ and 2*

While dissociation spectra for molecules in the $J''=1$ and 2 levels were observed (Fig. 9), these were of low intensity, because of the lower populations in these levels, and accurate values of the thresholds could not be determined. The spectrum for $J''=1$ exhibits an absorption just at the onset of the continuum and that for $J''=2$ appears to show a linear dependence of gradual slope over the first wave number above threshold, giving a value of $118\,850.68\pm0.09$ $cm^{-1}$. When the term value $F''(2)=179.029\pm0.004$ $cm^{-1}$ [21] is added, a value of $D_L(D_2)=119\,029.71\pm0.09$ $cm^{-1}$ is obtained for the second dissociation limit, confirming the more precise value obtained from the ortho-$D_2$ ($J''=0$) spectrum.

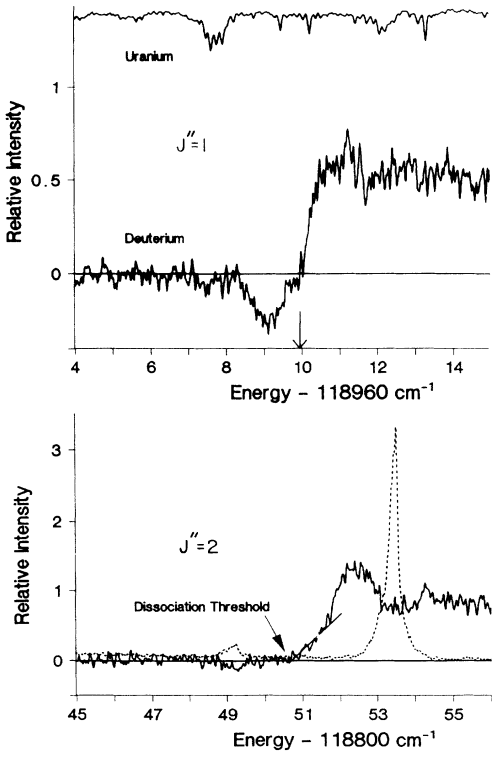


FIG. 9. Spectra of quenched fluorescence near the second dissociation limits of $D_2$ for $J''=1$ and 2. For $J''=2$ the spectrum recorded without a quenching field is shown by the dotted line.

### 3. *The dissociation energy $D_0(D_2)$ and $D_e(D_2)$ of deuterium*

In order to determine the dissociation energy of the ground electronic state, the $2s$-$1s$ energy interval of 82 281.336 $cm^{-1}$ [22] was subtracted from the $D_L(D_2)$ value for $J''=0$, namely, $119\,029.72\pm0.04$ $cm^{-1}$ to give

$$D_0(D_2)=36\,748.38\pm0.07\ cm^{-1}\ .$$

The addition of the zero-point energy $1546.49\pm0.05$ $cm^{-1}$ [20] leads to

$$D_e(D_2)=38\,294.87\pm0.09\ cm^{-1}\ .$$

## C. Sources of error

The precision quoted for the values of $D_0$ is based on the accuracy of the linear extrapolation of the intensity at the onset of dissociation (giving the value $D_L$), on the calibration of $2\nu_1$ and $\nu_2$, on a possible Doppler shift of the $H_2$ ($D_2$) spectrum, and on a small uncertainty in the $2s$-$1s$ interval in atomic hydrogen arising from hyperfine splitting.

### 1. *Linear extrapolation to the dissociation limit*

The dissociation continua of $H_2$ and $D_2$, recorded at the resolution of Figs. 6 and 8, both clearly show a steep rise in intensity from threshold, without extensive curvature at threshold. Therefore, extrapolation to the dissociation limit was carried out by excluding any apparent signal near threshold and fitting the main data to a straight line. The statistical errors in the fit determined the "extrapolation" error of $\pm0.04$ $cm^{-1}$ for both $H_2$ and $D_2$. The limits obtained by fitting slightly different portions of the data with lines of different slopes fell within this error. Next, the near-threshold part of each of the observed spectra was compared to the fit (after accounting for the spectral resolution) by translating the fitting line to higher and lower energies by an amount equal to the extrapolation error. It was found that any near-threshold contribution was contained within the resulting envelope of curves. Thus it seemed reasonable to assume that any deviations from linearity are either small or gradual, and not expected to be noticeable at the present sensitivity.

### 2. *Frequency calibration and ac Stark shift*

As already noted in Secs. III A 1 and III B 1, the uncertainties in the second dissociation limits $D_L(H_2)$ and $D_L(D_2)$ were $\pm0.04$ $cm^{-1}$. The uncertainty in $2\nu_1$ was discussed in Sec. II D and found to be $\pm0.04$ $cm^{-1}$. For $H_2$, the accuracy of $\nu_2$ was $\pm0.01$ $cm^{-1}$ and for $D_2\pm0.015$ $cm^{-1}$, as determined from fitting to the uranium spectrum. It may be mentioned that the measured value of $2\nu_1=94\,093.00\pm0.04$ $cm^{-1}$ is outside the uncertainty limits given in an earlier more precise measurement of the $4p^5 5p[\frac{1}{2}]_0$ energy level of $^{86}Kr$, namely, $94\,092.856\pm0.007$ $cm^{-1}$ [23]. The latter work was carried out at much lower intensities than used in the present dissociation experiments ($\sim 8\times10^8$ $W/cm^2$), thus indicating the occurrence of ac Stark shifts. Measure-

ments at different power of $\nu_1$ confirmed that this difference was due to a Stark shift of $(8.6\pm3.8)\times10^{-11}$ $cm^{-1}/W/cm^2$, and an extrapolation to zero intensity of $\nu_1$ gave a value of $2\nu_1=94\,092.93\pm0.05$ $cm^{-1}$, in essential agreement with the value of Ref. [23]. (A small isotope shift should be included since naturally occurring Kr used in the present work is predominantly $^{84}Kr$.) Nevertheless, for the present purposes, the frequency $2\nu_1=94\,093.00\pm0.04$ $cm^{-1}$ was used since it was the value obtained at the same intensity as used in the dissociation experiments. An uncertainty of $\pm0.03$ $cm^{-1}$ was included for a possible Stark shift of the Kr level arising from the small differences in beam profiles, and therefore of intensities, of the two different lasers used to calibrate $\nu_1$ and to photodissociate the $H_2$ and $D_2$. No Stark shift was detectable for radiation at $\nu_2$ even at intensities as high as $2.6\times10^9$ $W/cm^2$.

### 3. *Doppler shift of $H_2$ in the jet*

The component of molecular motion along the axis of the exciting radiation will introduce a Doppler shift to the fluorescence-excitation spectrum, according to the usual relation $\delta\nu=(v/c)\nu_{XUV}\sin\theta$, where $\theta$ is the angle of deviation from the vertical axis of the jet. First, the beam velocity $v$ was determined experimentally. Doppler shifts of 0, $-0.24$, and $0.072$ $cm^{-1}$ were measured for the $H_2$ lines of Fig. 7 as the jet was moved 0, $+1.13$, and $-0.75$ cm, respectively, along the laser beam direction. Since the jet expansion is conical, these positions correspond to $\theta=0$, 12.7°, and $-8.5$°, respectively. The resulting value for the vertical beam velocity was found to be $v=(2.1\pm0.3)\times10^3$ m/s.

A measurement of the deviation angle in the dissociation experiment yielded $0.58°\pm0.2°$, with the uncertainty increased to $\pm0.9°$ (or arctan 0.8/50) since the mirror in the $H_2$ chamber could drift its aim by at most 0.8 mm at the excitation region, 50 mm below the jet nozzle. Thus the Doppler shift was $+0.008\pm0.01$ $cm^{-1}$ for $H_2$ and $+0.006\pm0.008$ $cm^{-1}$ for $D_2$. All of the spectra were corrected for these shifts and the uncertainties were included in the quoted errors for dissociation energies.

### 4. *Uncertainty arising from 1s hyperfine splitting*

Hyperfine splitting of the photofragments introduces uncertainty in the $2s$-$1s$ energy interval used to determine $D_0$ from the second dissociation limit. This splitting is 0.047 $cm^{-1}$ for the $1s$ state of hydrogen and negligible for the $2s$ state of hydrogen and for both $1s$ and $2s$ states of deuterium. In an earlier publication [4], we assumed an uncertainty of 0.024 $cm^{-1}$ (or half the $1s$ splitting). However, by considering the symmetry of molecular wave functions involved in the photodissociation process and conservation of angular momentum, the uncertainty in the photofragment energy can be halved to $\pm0.013$ $cm^{-1}$ [24].

### 5. *Summary of uncertainties in $D_0(H_2)$ and $D_0(D_2)$*

A summary of the experimental uncertainties in determining the values of $D_0(H_2)$ and $D_0(D_2)$ is given in Table II. For both $H_2$ and $D_2$, the error in extrapolation to the second dissociation limit was the same, namely, $\pm0.04$ $cm^{-1}$. To this uncertainty were added, in quadrature, the uncertainties in calibration of $2\nu_1$ and $\nu_2$, in the ac Stark shift, and in the Doppler shift. Finally an uncertainty arising from the hyperfine splitting was added linearly for $H_2$. Thus experimental precisions of $\pm0.08$ and $\pm0.07$ $cm^{-1}$ were deduced for $D_0(H_2)$ and $D_0(D_2)$, respectively.

## IV. DISCUSSION AND CONCLUSIONS

We have used fluorescence excitation spectroscopy of the $B'\,^1\Sigma_u^+-X\,^1\Sigma_g^+$ transition to probe the region of the second dissociation limit in hydrogen and deuterium. The onset of photodissociation has been observed clearly for both molecules, and the thresholds measured directly. The experimental conditions ensure that only the photofragments H($2s$) and D($2s$) contribute to the observed dissociation spectra. Consequently, the dissociation energies $D_0(H_2)$ and $D_0(D_2)$ for the ground electronic states could be determined with a precision better than $\pm0.10$ $cm^{-1}$. These values are in good agreement with the most recent *ab initio* calculations [2], which include radiative, relativistic, and nonadiabatic corrections.

There are several experimental determinations of $D_0(H_2)$ and $D_0(D_2)$ with which to compare our values (Table III). The most recent are those of Eyler and Melikechi [9], who applied a different experimental technique, namely, double-resonance spectroscopy, to probe the same excited states of $H_2$ and $D_2$. They obtained $D_0(H_2)=36\,118.06\pm0.04$ $cm^{-1}$ and $D_0(D_2)=36\,748.32\pm0.07$ $cm^{-1}$. These results are in good agreement with ours of $36\,118.11\pm0.08$ and $36\,748.38\pm0.07$ $cm^{-1}$, respectively, and are of comparable accuracy. This agreement is reassuring considering the differences in the two

TABLE II. Experimental uncertainties in the determination of $D_0(H_2)$ and $D_0(D_2)$ in $cm^{-1}$.

| Source | Hydrogen | Deuterium |
|---|---|---|
| Extrapolation to $D_L$ | 0.04 | 0.04 ($J''=0$)<br>0.09 ($J''=2$) |
| Calibration of $\nu_2$ | 0.01 | 0.015 ($J''=0$)<br>0.01 ($J''=2$) |
| Calibration of $2\nu_1$ | 0.04 | 0.04 |
| ac Stark shift | 0.03 | 0.03 |
| Doppler shift | 0.01 | 0.008 |
| Hyperfine splitting correction | 0.013 | 0.0 |

TABLE III. Recent experimental evaluations and *ab initio* calculations of $D_0(H_2)$, $D_0(D_2)$, and $D_0(H_2^+)$, and $D_0(D_2^+)$ in $cm^{-1}$.

| | $H_2$ | $D_2$ | Authors |
|---|---|---|---|
| Experiment | 36 118.3 | 36 748.9±0.4 | Herzberg [5] |
| Experiment | 36 118.6±0.5 | | Stwalley [6] |
| Experiment | | 36 748.88±0.3 | LeRoy and Barwell [7] |
| Experiment | 36 118.26±0.20 | | McCormack and Eyler [3] |
| Experiment | 36 118.06±0.04 | 36 748.32±0.07 | Eyler and Melikechi [9] |
| Experiment | 36 118.11±0.08 | 36 748.38±0.07 | Present [4,10] |
| Theory | 36 118.060±0.01 | 36 748.355±0.01 | Wolniewicz [2] |
| Theory | 36 118.088±0.1 | 36 748.347±0.1 | Kolos, Szalewicz, and Monkhorst [2] |
| | $H_2^+$ | $D_2^+$ | Authors |
| Experiment | 21 379.37±0.08 | 21 711.64±0.07 | Present [10] |
| Theory | 21 379.348 | 21 711.580 | Wolniewicz and Orlikowski [31] |

experimental techniques. It may also be mentioned that there is similar good agreement for the dissociation energy of HD. Eyler and Melikechi [9] obtained 36 405.88±0.10 $cm^{-1}$, and Balakrishnan, Vallet, and Stoicheff [25], using the same technique described here, found 36 405.83±0.10 $cm^{-1}$. Both experimental values compare very well with the calculated value of 36 405.774±0.01 $cm^{-1}$ given by Wolniewicz [2].

As already noted, the accuracy of the present results was affected by various sources of error, namely, extrapolation to the second dissociation limit, calibration of laser frequencies, and the uncertainties in the ac Stark shift and the Doppler shift. Each of these were of similar magnitude. While in principle there is no fundamental limit to the precision possible with the present technique, many experimental changes would be necessary to significantly improve the final accuracy, and this task may be formidable. In particular, the linear dependence of the onset of photodissociation for both $H_2$ and $D_2$ (clearly evident in Figs. 6 and 8) is not the expected envelope. A calculation of the cross section for dissociation of the $B'$ state has been performed by Zucker and Eyler [26], and they predicted that the near-threshold intensity should increase in accordance with the Wigner threshold law. That is, for $H_2(J''=1)$ the intensity should increase as $E^{1/2}$, with $E$ the energy above threshold, and for $D_2(J''=0)$ as $E^{3/2}$. Since the present results do not appear to follow this prediction, greater resolution or higher signal-to-noise ratio than that obtained here may be needed to test the threshold law in this application.

The consistency of the present results was tested in comparison with high-precision measurements of the related ionization potentials $I(H)$ and $I(H_2)$ made in other laboratories, and at the same time values for the dissociation energies of the molecular ions $H_2^+$ and $D_2^+$ were deduced. From Fig. 10 it is readily found that

$$D_0(H_2^+)=D_0(H_2)+I(H)-I(H_2)\ ,$$

and similarly for deuterium. Gilligan and Eyler [27] obtained the value $I(H_2)=124\,417.507\pm0.018$ $cm^{-1}$ and Jungen *et al.* [28] 124 417.484±0.017 $cm^{-1}$. (Both values rely on a measurement by the first group and incorporate a recent change reported by them.) The average of these two values is $I(H_2)=124\,417.500\pm0.01$ $cm^{-1}$. For atomic hydrogen, $I(H)=109\,678.764\pm0.01$ $cm^{-1}$ [29]. Thus $D_0(H_2^+)=21\,379.37\pm0.08$ $cm^{-1}$. In a similar manner, using $I(D_2)=124\,745.353\pm0.024$ $cm^{-1}$, and $I(D)=109\,708.617$ $cm^{-1}$ from Jungen *et al.* [28,30], we find $D_0(D_2^+)=21\,711.64\pm0.07$ $cm^{-1}$.

These experimentally derived values for the dissociation energies of the $H_2^+$ and $D_2^+$ ions are also in good agreement with recent *ab initio* calculations [31], namely 21 379.348 and 21 711.580 $cm^{-1}$, respectively. This agreement is gratifying in several ways. First, the measurements of $I(H_2)$ and $I(D_2)$ were performed in two different laboratories, using altogether different techniques. Thus these different experiments are shown to be consistent with each other. Second, it appears that the theoretical calculations for the neutral molecules and for the molecular ions are also consistent with each other. The ions are comprised of only three particles and the Hamiltonian governing their properties is much simpler than that for $H_2$ or $D_2$, so that the binding energies of the molecular ions have been calculated to better than ±0.01

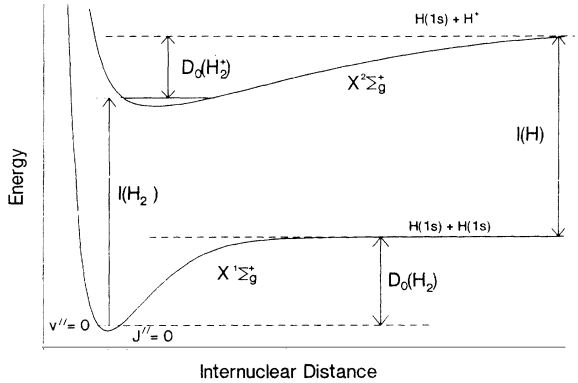


FIG. 10. Energy-level diagram of $H_2$ and $H_2^+$ describing the determination of $D_0(H_2^+)$ from $D_0(H_2)$ and the ionization potentials of H and $H_2$.

$cm^{-1}$. Finally, the good agreement of the derived and calculated values essentially confirms the evaluation and accuracy of $D_0(H_2)$ and $D_0(D_2)$ in the present experiments.

In summary, the present investigation and that of Eyler and Melikechi [9] have solved a fundamental problem in molecular spectroscopy, the determination of the dissociation energies of the simplest molecules, with an accuracy sufficient to test the most recent theoretical calculations.

## ACKNOWLEDGMENTS

This research was supported by the Natural Sciences and Engineering Research Council (NSERC), the Ontario Technology Fund, and the University of Toronto. A.B. is grateful to the University of Toronto and NSERC, and V.S. to the Ministère des Affaires Etrangères (France) and the National Research Council (Canada) for financial support during the course of this research. We thank D. Warwick for advice and technical assistance.

[1] G. Herzberg and A. Monfils, J. Mol. Spectrosc. **5**, 482 (1960).
[2] L. Wolniewicz, J. Chem. Phys. **99**, 1851 (1993); see also W. Kolos, K. Szalewicz, and H. J. Monkhorst, *ibid.* **84**, 3278 (1986).
[3] E. F. McCormack and E. E. Eyler, Phys. Rev. Lett. **66**, 1042 (1991); E. E. Eyler, Comments At. Mol. Phys. **24**, 299 (1990); E. F. McCormack, Ph.D. thesis, Yale University, 1989.
[4] A. Balakrishnan, V. Smith, and B. P. Stoicheff, Phys. Rev. Lett. **68**, 2149 (1992).
[5] G. Herzberg, J. Mol. Spectrosc. **33**, 147 (1970); Comment. Pontif. Acad. Sci. **2**, 1 (1972).
[6] W. C. Stwalley, Chem. Phys. Lett. **6**, 241 (1970).
[7] R. J. LeRoy and M. G. Barwell, Can. J. Phys. **53**, 1983 (1975).
[8] H. Bredohl and G. Herzberg, Can. J. Phys. **51**, 867 (1973).
[9] E. E. Eyler and N. Melikechi, Phys. Rev. A **48**, R18 (1993).
[10] A. Balakrishnan and B. P. Stoicheff, J. Mol. Spectrosc. **156**, 517 (1992).
[11] E. E. Witmer, Phys. Rev. **28**, 1223 (1926).
[12] W. Heitler and F. London, Z. Phys. **44**, 455 (1927).
[13] M. G. Littman, Opt. Lett. **3**, 138 (1978).
[14] M. G. Littman, Appl. Opt. **23**, 4465 (1984).
[15] R. T. Hodgson, P. P. Sorokin, and J. J. Wynne, Phys. Rev. Lett. **32**, 343 (1974); W. Jamroz and B. P. Stoicheff, in *Progress in Optics XX*, edited by E. Wolf (North-Holland, Amsterdam, 1983), pp. 325–380; C. R. Vidal, in *Tunable Lasers*, edited by L. F. Mollenauer and J. C. White (Springer-Verlag, Berlin, 1987), pp. 57–113.
[16] G. Hilber, A. Lago, and R. Wallenstein, J. Opt. Soc. Am. B **4**, 1753 (1987).
[17] B. A. Palmer, R. A. Keller, and R. Engleman, Los Alamos Scientific Laboratory Report No. LA-8251-MS, UC-34a, 1980 (unpublished).
[18] J. V. Foltz, D. H. Rank, and T. A. Wiggins, J. Mol. Spectrosc. **21**, 203 (1966).
[19] T. Andreae, W. König, R. Wynands, D. Leibfreid, F. Schmidt-Kaler, C. Zimmermann, D. Meschede, and T. W. Hänsch, Phys. Rev. Lett. **69**, 1923 (1992).
[20] K. P. Huber and G. Herzberg, *Molecular Spectra and Molecular Structure; Constants of Diatomic Molecules* (Van Nostrand Reinhold, Toronto, 1979).
[21] P. J. Brannon, C. H. Church, and C. W. Peters, J. Mol. Spectrosc. **27**, 44 (1968).
[22] M. G. Boshier, P. E. G. Baird, C. J. Foot, E. A. Hinds, M. D. Plimmer, D. N. Stacey, J. B. Swan, D. A. Tate, D. M. Warrington, and G. K. Woodgate, Nature **330**, 463 (1987).
[23] T. Trickl (private communication); T. Trickl, M. J. J. Vrakking, E. Cromwell, Y. T. Lee, and A. H. Kung, Phys. Rev. A **39**, 2948 (1989).
[24] A. Balakrishnan, Ph.D. thesis, University of Toronto, 1993, pp. 74–76.
[25] A. Balakrishnan, M. Vallet, and B. P. Stoicheff, J. Mol. Spectrosc. **162**, 168 (1993).
[26] C. W. Zucker and E. E. Eyler, J. Chem. Phys. **85**, 7100 (1986).
[27] J. M. Gilligan and E. E. Eyler, Phys. Rev. A **46**, 3676 (1992).
[28] Ch. Jungen, I. Dabrowski, G. Herzberg, and M. Vervloet, J. Chem. Phys. **93**, 2289 (1990).
[29] G. W. Erickson, J. Phys. Chem. Ref. Data **6**, 831 (1977).
[30] Ch. Jungen, I. Dabrowski, G. Herzberg, and M. Vervloet, J. Mol. Spectrosc. **153**, 11 (1992).
[31] L. Wolniewicz and T. Orlikowski, Mol. Phys. **74**, 103 (1991).